

Accommodating sodium into three-dimensional hosts with a nanoscale sodophilic layer towards stable pre-stored Na metal anodes

Juli Liang, Wenwei Wu, Yang Chao, Yilong Li, Junfei Wu, Yulu Xie, Xuehang Wu*

Guangxi Key Laboratory of Processing for Non-ferrous Metals and Featured Materials, School of Chemistry and Chemical Engineering, Guangxi University, Nanning 530004, PR China

Corresponding author. E-mail: xhwu@gxu.edu.cn (X. Wu)

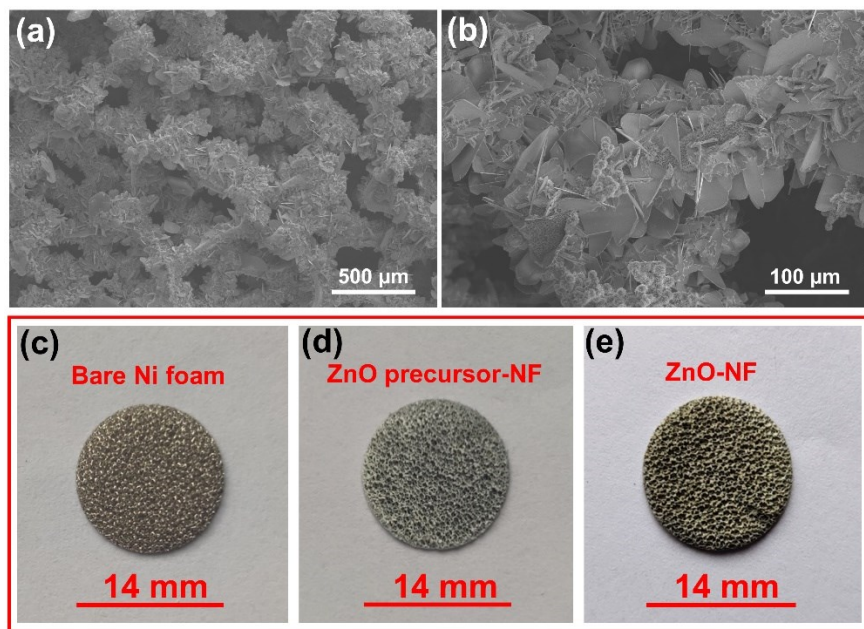


Fig. S1. (a,b) SEM images of ZnO precursor-NF. Digital images of (c) bare Ni foam, (d) ZnO precursor-NF, and (e) ZnO-NF.

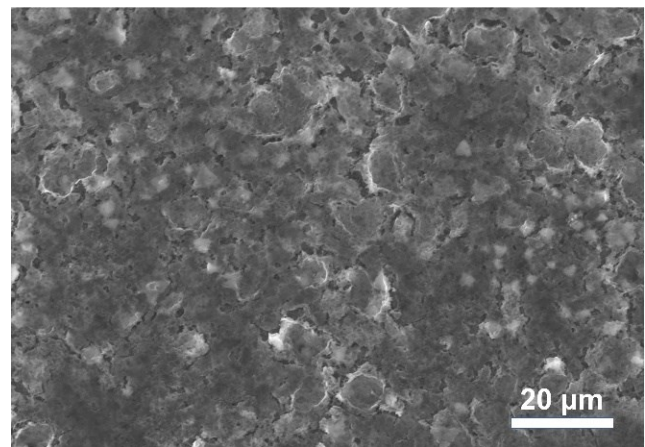


Fig. S2. SEM image of Na-NF.

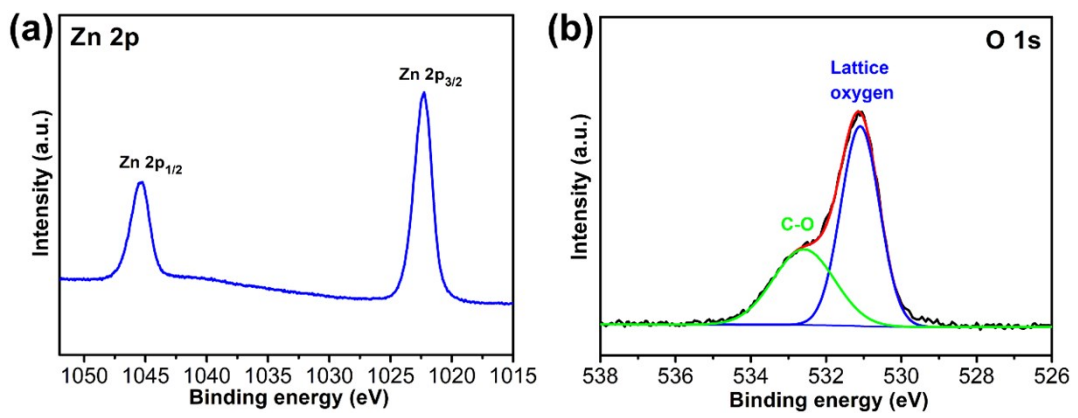


Fig. S3. High-resolution (a) Zn 2p and (b) O 1s XPS spectra of ZnO-NF.

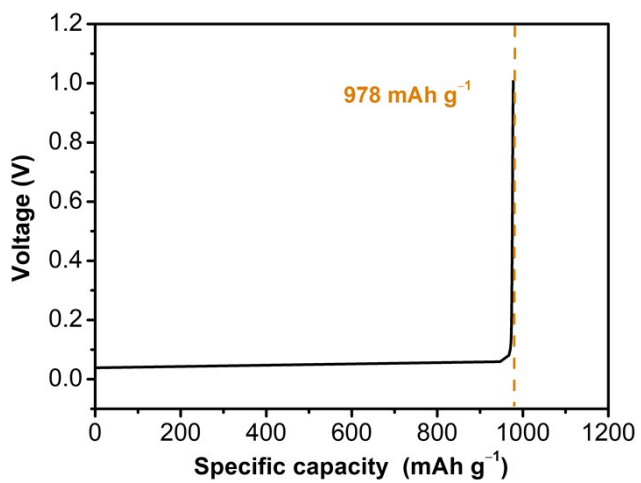


Fig. S4. Galvanostatic stripping voltage profile of Na-Zn-NF. The current density was 1 mA cm⁻² and the cut-off voltage was 1.0 V.

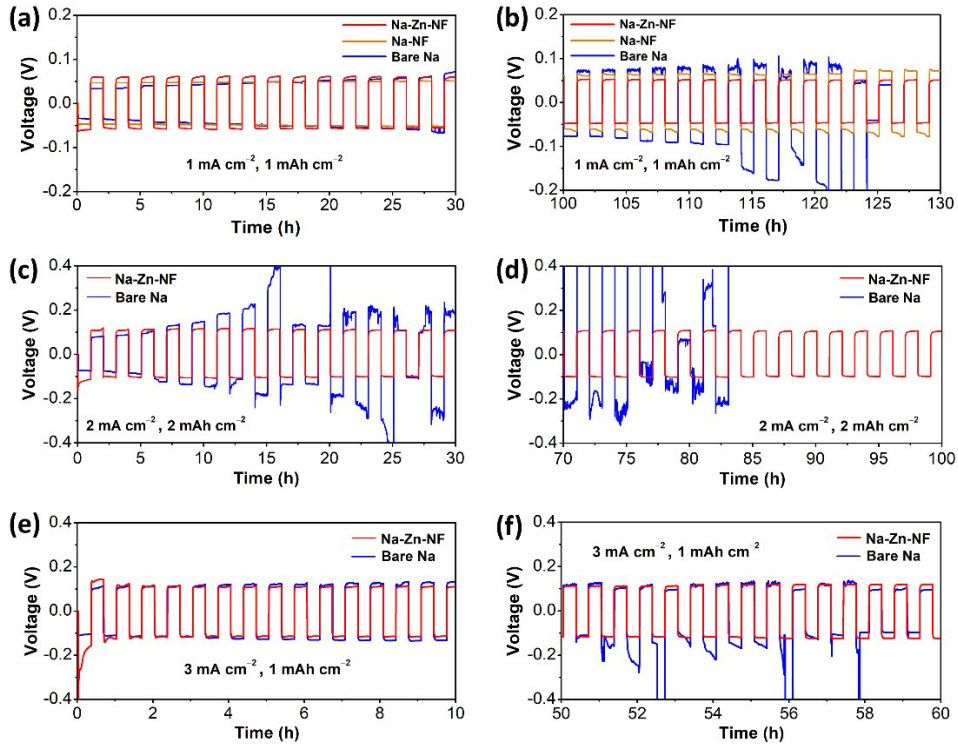


Fig. S5. (a,b) Enlarged voltage profiles of the Na-Zn-NF, Na-NF, and bare Na symmetric cells at a current density of 1 mA cm^{-2} with a capacity of 1 mAh cm^{-2} . Enlarged voltage profiles of the Na-Zn-NF and bare Na symmetric cells (c,d) at a current density of 2 mA cm^{-2} with a capacity of 2 mAh cm^{-2} and (e,f) at a current density of 3 mA cm^{-2} with a capacity of 1 mAh cm^{-2} .

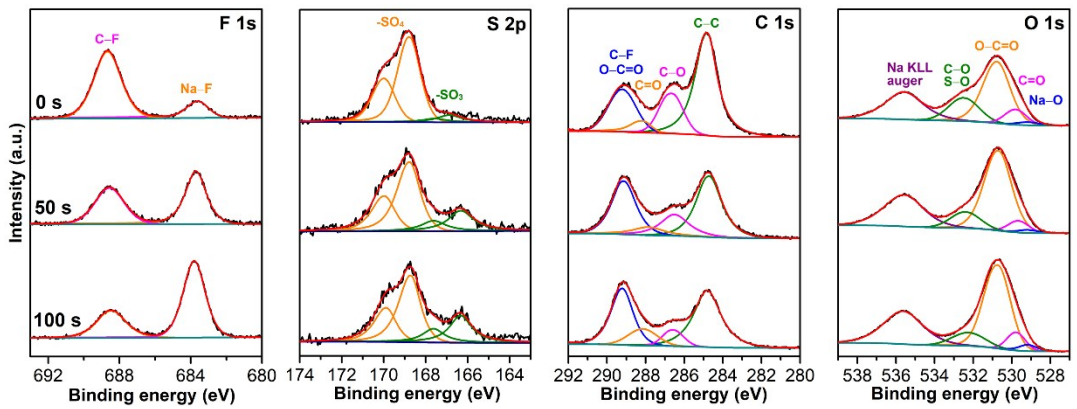


Fig. S6. F 1s, S 2p, C 1s, and O 1s XPS spectra of the cycled Na-NF before (0 s) and after etching for 50 s and 100 s.

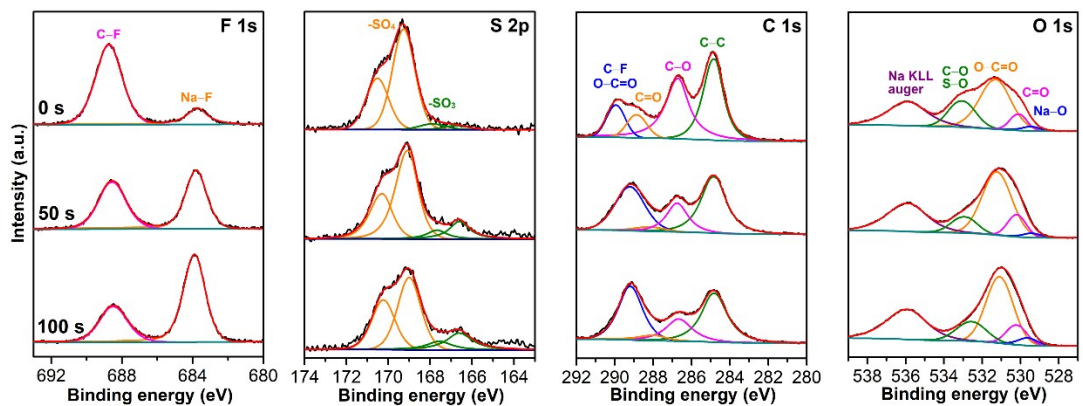


Fig. S7. F 1s, S 2p, C 1s, and O 1s XPS spectra of the cycled bare Na before (0 s) and after etching for 50 s and 100 s.

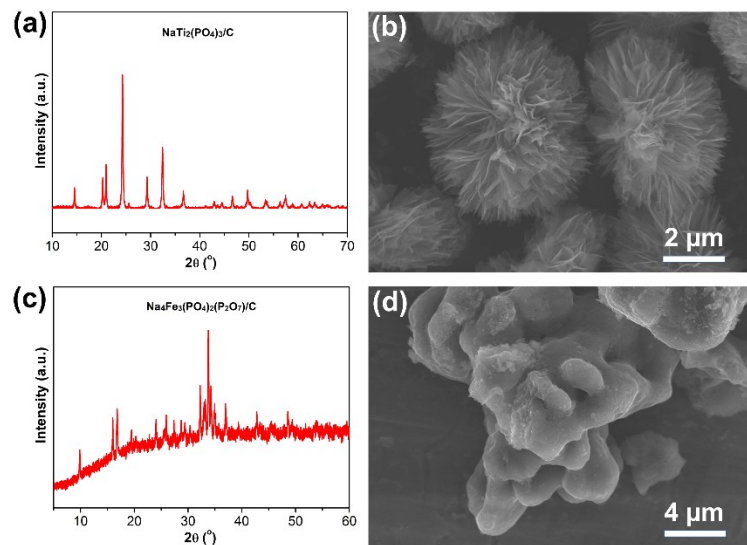


Fig. S8. (a) XRD pattern and (b) SEM image of $\text{NaTi}_2(\text{PO}_4)_3/\text{C}$. (c) XRD pattern and (d) SEM image of $\text{Na}_4\text{Fe}_3(\text{PO}_4)_2(\text{P}_2\text{O}_7)/\text{C}$.

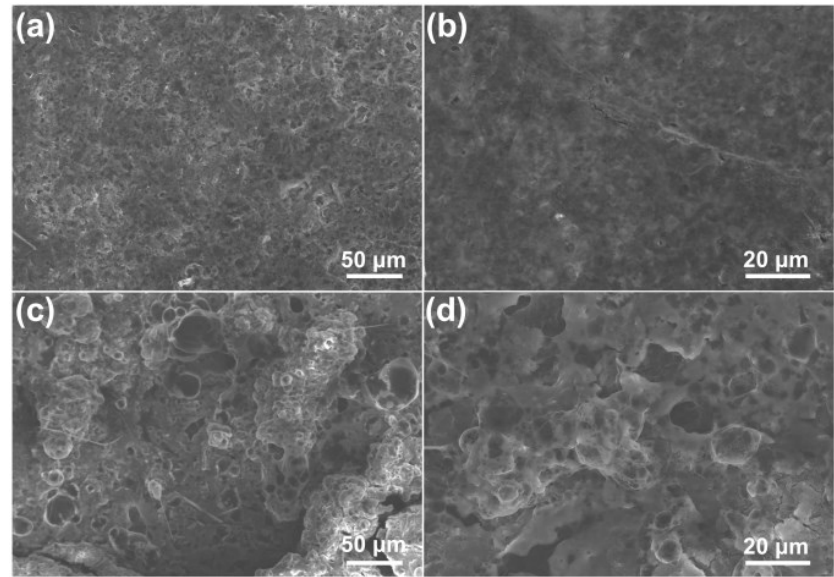


Fig. S9. SEM images of the Na-Zn-NF after 1000 cycles and the bare Na after 600 cycles in full cells.

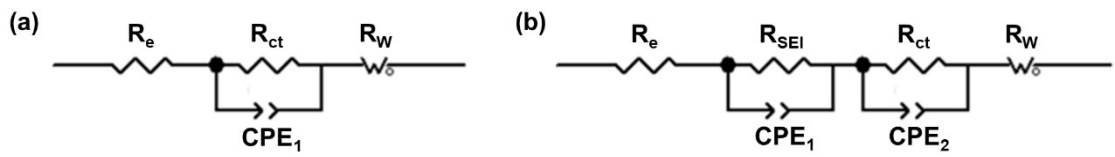


Fig. S10. Equivalent circuits used to fit the Nyquist plots of the Na-Zn-NF, Na-NF, and bare Na symmetric cells (a) before and (b) after 50 cycles.

Table S1. Masses of ZnO-NF, Na-Zn-NF, and Na in Na-Zn-NF. Three representative

	ZnO-NF	Na-Zn-NF	Na in Na-Zn-NF
Sample 1	53.1 mg	102.4 mg	49.3 mg
Sample 2	53.4 mg	103.1 mg	49.7 mg
Sample 3	53.3 mg	102.7 mg	49.4 mg
Average	53.3 mg	102.7 mg	49.5 mg

groups of samples are selected.

Table S2. Comparison of cycling performance between Na-Zn-NF and other state-of-the-art Na metal anodes.

Materials	Capacity (mAh cm ⁻²)	Current density (mA cm ⁻²)	Cycles	Time (h)	Electrolyte	Ref.
Na-Zn-NF	1	1	> 1000	> 2000	1 M NaCF₃SO₃ in diglyme	This work
	2	2	> 550	> 1100		
Na carbonized wood	1	1	> 250	> 500	1 M NaClO ₄ in EC/DEC	1
Na/Ni foam	1	1	> 300	> 600	1 M NaPF ₆ in DEGDME	2
Na@oxygen-treated Cu foam	1	0.5	> 100	> 400	1 M NaClO ₄ in EC/DEC	3
Na/3D flexible carbon Felt	2	1	> 120	> 480	1 M NaClO ₄ in EC/PC	4
Na@CP-NCNTs	1	1	> 175	> 350	1 M NaPF ₆ in EC/PC	5
	1	3	> 270	> 180		
Na-carbon cloth composite	1	1	> 100	> 200	1 M NaCF ₃ SO ₃ in DME	6
Na-carbon fiber	1	0.5	> 150	> 300	1 M NaClO ₄ in EC/DMC/EMC with 5% FEC	7
Na-Sn alloy/Na ₂ O	1	1	> 350	> 700	1 M NaCF ₃ SO ₃ in diglyme	8
	1	2	> 500	> 500		
Na-Na ₂ S-carbonized tissue paper	0.5	1	> 300	> 300	NaClO ₄ in EC/DEC with 10% FEC	9

Table S3. Percentages of F, S, C, and O elements detected at different depths of SEI films on the cycled Na-Zn-NF, Na-NF, and bare Na.

Electrodes	Etching time (s)	Percentages (%)			
		F	S	C	O
Na-Zn-NF	0	11.82	3.30	16.70	68.18
	50	9.49	3.22	13.20	74.09
	100	9.82	3.11	12.31	74.76
Na-NF	0	11.98	2.77	19.28	65.97
	50	11.47	2.65	15.21	70.67
	100	12.48	2.74	13.92	70.86
Bare Na	0	13.93	2.87	18.84	64.36
	50	14.14	3.04	14.57	68.25
	100	15.45	2.92	13.13	68.50

References

- 1 W. Luo, Y. Zhang, S. Xu, J. Dai, E. Hitz, Y. Li, C. Yang, C. Chen, B. Liu and L. Hu, Encapsulation of metallic Na in an electrically conductive host with porous channels as a highly stable Na metal anode, *Nano Lett.*, 2017, **17**, 3792–3797.
- 2 Q. Lu, X. Wang, A. Omar and D. Mikhailova, 3D Ni/Na metal anode for improved sodium metal batteries, *Mater. Lett.*, 2020, **275**, 128206.
- 3 C. Wang, H. Wang, E. Matios, X. Hu and W. Li, A chemically engineered porous copper matrix with cylindrical core-shell skeleton as a stable host for metallic sodium anodes, *Adv. Funct. Mater.*, 2018, **28**, 1802282.
- 4 S. S. Chi, X. G. Qi, Y. S. Hu and L. Z. Fan, 3D flexible carbon felt host for highly stable sodium metal anodes, *Adv. Energy Mater.*, 2018, **8**, 1702764.
- 5 Y. Zhao, X. Yang, L. Y. Kuo, P. Kaghazchi, Q. Sun, J. Liang, B. Wang, A. Lushington, R. Li, H. Zhang and X. Sun, High capacity, dendrite-free growth, and minimum volume change Na metal anode, *Small*, 2018, **14**, 1703717.
- 6 W. Go, M. H. Kim, J. Park, C. H. Lim, S. H. Joo, Y. Kim and H. W. Lee, Nanocrevasse-rich carbon fibers for stable lithium and sodium metal anodes, *Nano Lett.*, 2019, **19**, 1504–1511.
- 7 Y. Zhang, C. Wang, G. Pastel, Y. Kuang, H. Xie, Y. Li, B. Liu, W. Luo, C. Chen and

L. Hu, 3D wettable framework for dendrite-free alkali metal anodes, *Adv. Energy Mater.*, 2018, **8**, 1800635.

8 X. Zheng, W. Yang, Z. Wang, L. Huang, S. Geng, J. Wen, W. Luo and Y. Huang, Embedding a percolated dual-conductive skeleton with high sodiophilicity toward stable sodium metal anodes, *Nano Energy*, 2020, **69**, 104387.

9 W. Wu, S. Hou, C. Zhang and L. Zhang, A dendrite-free Na-Na₂S-carbon hybrid toward a highly stable and superior sodium metal anode, *ACS Appl. Mater. Interfaces*, 2020, **12**, 27300–27306.